Continuous decontamination of metal-polluted mine water using engineered hybrid adsorbent

AM. Muliwa, MS. Onyango, A. Maity and A. Ochieng

***Abstract*-** Mining industries contribute enormously to water pollution through discharge of effluents contaminated with metals. Metals-polluted water is a threat to aquatic and human lives as well as the general ecosystem. Numerous conventional treatment methods are available for the removal of metals from mine water, but majority of them are costly, inefficient for trace metal concentration, and generate voluminous secondary sludge. Therefore, there is need for alternative low-cost novel technologies capable of reducing metal concentration in water to acceptable levels. Adsorption technology is increasingly receiving preference because it is simple in design, requires low initial cost, easy to operate, can remove contaminants in trace levels and the possibility to develop and employ wide variety of adsorbents. This study, therefore, explored the removal of manganese [Mn (II)] from aqueous solution using a bentonite/metal oxide hybrid ($B/MeO_x/H$) hydrogels adsorbent packed in a fixed-bed reactor. The adsorption performance was examined by breakthrough behaviors under various experimental conditions such as bed height and influent flow rate. It was found that increase in bed height resulted to increase in both breakthrough and saturation times, while it was opposite with influent flow rate. The breakthrough curves were characterized by slightly flatter breakthrough curves for large bed depth and low flow rate. The overall adsorption performance of the fixed-bed column highly depended on the operating parameters. The experimental breakthrough data was sufficiently described by Yoon-Nelson model. Bed depth service time (BDST) predicted well the breakthrough times for different flow rates. The findings demonstrate that $B/MeO_x/H$ hydrogel adsorbent could effectively polish mine water laded with trace concentration of Mn (II).

***Keywords*—**Adsorption, Breakthrough, Hybrid, Mine water

1. Introduction

Water pollution by manganese (Mn) mainly results from the disposal of partially treated effluents from electroplating, mining, coal and oil burning battery manufacturing, chemical manufacturing, and metal alloying industries, among others, into municipal sewers [1]. Elevated concentration of Mn is detrimental to both living organisms and the general environment. Under normal environmental conditions, the divalent form [Mn (II)] is the most stable and predominates over a wide range of pH. Due to Mn (II) toxicity and non-biodegradability, there is urgent need for innovative technologies capable of removing Mn (II) from industrial effluent to acceptable standards [2]. Conventional treatment methods of Mn(II)-contaminated waters include chemical precipitation, ion-exchange, membrane filtrations, biological methods and adsorption etc. Precipitation is highly commercialised but, the requisite to raise the pH above 10, so as to comply with the discharge limits, is a problem for discharging [3].

Adsorption technique has attracted a lot of attention because it is simple, non-toxic, and suitable for trace level contaminants concentrations and does not generate secondary waste. Moreover, adsorption technology is flexible and can be integrated into an existing treatment system to achieve complete metal ions removal [4]. Several adsorbents have been reported for metal ions removal from aqueous solutions. However, there is growing interest in low-cost adsorbent (LCAs) materials as they are cheap, surface-modifiable to enhance adsorption capacity and selectivity, and they can be regenerated for re-use [5]. Among these LCAs, bentonite has shown promising results with regard to environmental clean-up, thanks to its high cation exchange capacity, layered structure, increased surface area, and swelling characteristic which enables them retain contaminants within the structure [6]. However, bentonite still exhibit low capacities for metal ions, stickiness and poor chemical and mechanical properties. In order to improve the adsorption performance of bentonite, it is important to physically or chemically modify their surfaces [7].

Metal oxides are widely known as efficient scavengers of metal ions [8] and could serve as modifying agents of bentonite. Metal oxides would not only provide reactive surface for metal removal, but also densify bentonite and improve the dispersion characteristics of the resultant adsorbent. However, both bentonite and metal oxides are usually available in powder form, making them unsuitable for application in continuous fixed-bed adsorption. Fixed-bed columns packed with powdered adsorbents suffer from high pressure drops, thus particles of appropriate sizes should be used. Consequently, in this study, manganese oxides (MeO_x) were immobilized on bentonite (B) surface and bound on chitosan to produce hydorgels for Mn (II) adsorptions. The

A.M. Muliwa, MS Onyango, Department of Chemical, Metallurgical and Materials Engineering, Tshwane University of Technology (corresponding author phone: +27818445644; fax: +27123823550; e-mail: amuliwa@yahoo.com).

A. Maity, DST/CSIR National Centre for Nanostructured Materials, Council for Scientific and Industrial Research, Pretoria.

A. Ochieng, Centre for Renewable Energy and Water, Vaal University of Technology, South Africa

choice of MeO_x was guided by the fact that they have demonstrated superior adsorption performance towards metal ions than other metal oxides, attributable large porosity, high catalytic activity and large surface areas [9]. Furthermore, chitosan being biocompatible and non-toxic polymer was chosen as a binder. The resultant adsorbent (B/MeOx/H) was examined for the sequestration of Mn (II) using a continuous fixed-bed operation. The influence of various process variables on Mn (II) breakthrough curves was explored. Finally, experimental breakthrough data was fitted with Yoon-Nelson, Adams-Bohart and bed depth service time (BDST) models to predict the performance under different conditions.

2. Materials and Methods

2.1. Adsorbent preparation and characterization

The hydrogels were prepared as follows: First, 0.2M permanganate solution was prepared and heated to boiling at 90ºC. Then, 2 g of bentonite powder was added and the mixture was stirred vigorously for 10 min. Next, 5 mL hydrochloric acid (32% m/v) was titrated into the mixture and a brown suspension was formed. The mixture was further maintained at 90ºC for 1 h, after which it was allowed to cool naturally. Thereafter, the brown solids were vacuum filtered and dried at 100ºC for 24 h. Separately, 1g of chitosan flakes was dissolved in 100 mL of 5% glacial acetic acid until a gel was formed. To this, 1 g of the brown-dried powder from the first experiment was added and the mixture was stirred for 30 min to achieve homogeneity. The resulting mixture was then added dropwise into 0.2M NaOH solution using a syringe tube. Consequently, spherical hydrogels were formed through coagulation and were left in the NaOH solution overnight under soaking. Finally, the brown hydrogels were recovered and washed thoroughly with plenty of water, air-dried and labelled B/MeO_x/H, awaiting further use.

2.2. Continuous decontamination studies

Figure 1 shows the fixed-bed experimental set-up used in this study.

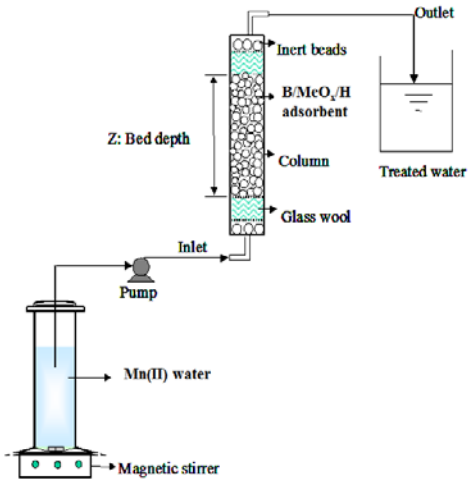

Fig. 1. Fixed-bed adsorption column experimental set-up

A Perspex column with 2 cm internal diameter and 30 cm length was used for experiments. B/MeOx/H hydrogels were placed in the middle of the column tube supported on either side by inert glass beads and glass wool. Mn (II) water was pumped in an upward fashion using a peristaltic pump and effluent samples were collected at predetermined time intervals.

The effect of process parameters such as bed depth (20, 30 and 40 mm) and influent flowrate (1.67, 3.33 and 5.1 mL/min) on breakthrough curves (BTC) was investigated. For the effect of bed depth, the influent concentration of Mn (II) and flow rate were kept constant at 50 mg/L and 3.33 mL/min, respectively. On the other hand, the effect of influent flow rate was explored by fixing bed depth at 20 mm and influent concentration at 50 mg/L. In both experimental runs, samples were collected periodically from the column exit and were analyzed for Mn (II) using inductively coupled plasma optical emission spectrometer (ICP, 9000 Shimadzu). Then breakthrough curves were constructed by plotting C_t/C_o versus time, *t*, whereby C_t is the effluent concentration at any given time and C_o is the influent concentration.

3. Results and Discussion

3.1. Adsorbent characterization

Figure 2 (a) shows SEM image of B/MeOx/H hydrogel bead at x50 magnification while Fig. 2 (b) shows the corresponding EDX spectra. The bead appears almost spherical with a rough surface, which an important feature in adsorption application as it exposes large contact surface area between the adsorbate and the adsorbent. The EDX spectra confirms the presence of all elements representing the individual components making up the hydrogel. Si, K, Al, Ca and Na, represent bentonite, Mn and O peaks confirms the presence of manganese oxides.

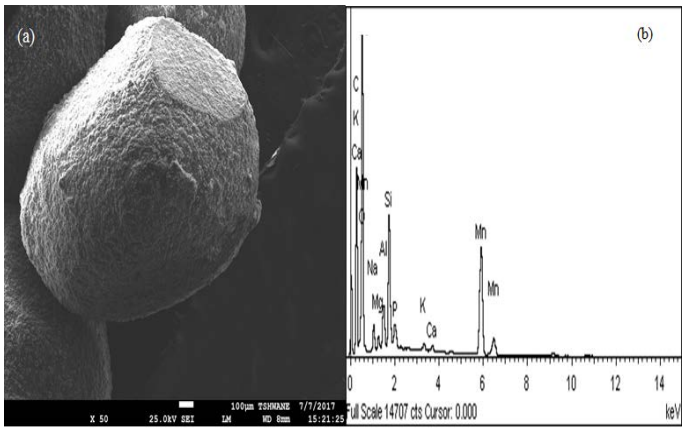

Fig. 2. Scanning electron microscope images (a) and energy dispersive X-ray spectra (EDX) of B/MeO_x/H adsorbent

3.2. The effect of process variables on Mn (II) breakthrough curves

Process variable are known to affect the performance of any adsorption system. Therefore, in this study, the effect of bed depth and influent flow rate on Mn (II) breakthrough curves

were investigated. Figure 3 displays breakthrough profiles obtained for different bed depths. As can be seen, early breakthrough times are evident for shorter bed depths while delayed breakthrough times are characterized by longer bed depths. The same scenario is exhibited for bed saturation times. These results were ascribed to increased active sites available for Mn (II) adsorption for longer bed depths and vice versa [10]. Moreover, for a fixed flow rate, increase in bed depths results in longer residence time which enhances contact time between the adsorbate and the packed hydrogel material. Considering the nature of breakthrough behavior, 20 mm bed depth was utilized for further adsorption experiments.

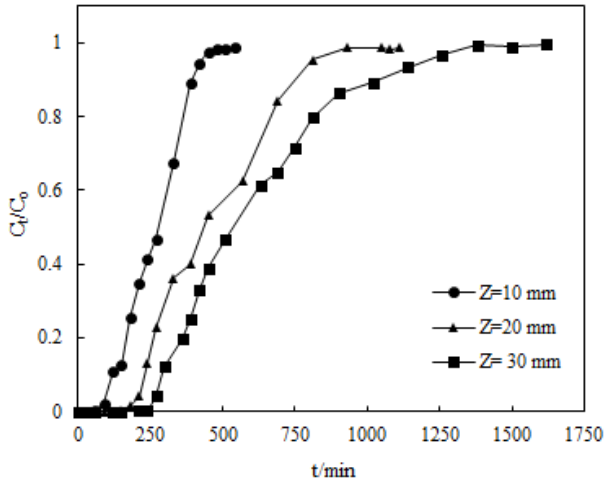

Fig. 3. Effect of bed depth on Mn (II) breakthrough behavior (C_o= 50 mg/L, Q=3.33 mL/min

The effect of influent flow rate on breakthrough curves was also explored and results are presented in Fig. 4.

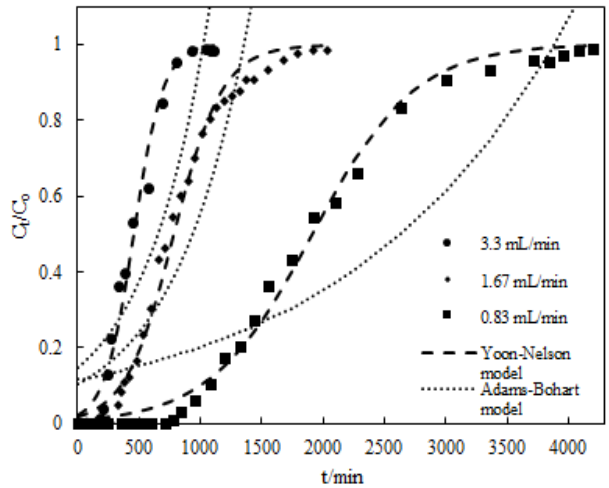

Fig. 4. Effect of influent flow rate on breakthrough curves and Yoon-Nelson and Adam-Bohart model fits (Z= 20 mm, C_o= 50 mg/L)

Contrary to the results on bed depth, increasing influent flow rate resulted in short breakthrough time while a decrease in flow rate produced delayed breakthrough curves. Further, for small flow rate, the breakthrough curves appeared elongated while at higher flow rates, sharper profiles were realized [11]. Early breakthroughs were attributed to less contact time and vice versa. These results indicate that less flow rates favor Mn (II) removal by B/MeOx/H hydrogels.

The experimental breakthrough data was further fitted with Yoon-Nelson model (Eq. (1)) and Adams-Bohart model (Eq. (2)) [12] to predict the adsorption capacity and possible mechanisms.

$$\ln\left(\frac{C_t}{C_o - C_t}\right) = k_{YN}t - k_{YN}\tau \quad (1)$$

where k_{YN} (min^{-1}) is the rate constant, τ (min) is the time required for 50% breakthrough, t (min) is the operation time.

$$\ln\left(\frac{C_t}{C_o}\right) = k_{BA}C_o t - k_{BA}N_o\frac{Z}{U} \quad (2)$$

where k_{BA} (L/mg.min) is the kinetic constant, N_o (mg/L) is the saturation concentration, Z (cm) is the bed depth, and U (cm/min) is linear velocity inside the fixed-bed.

For the two models, plots of the linear equations (not shown) were used to extract parameters from the slope and intercept, after which the obtained parameters were used to predict the non-linear fittings. Figure 4 shows sample model fitting with the influent flow rate. It is clear that the Yoon-Nelson model followed the breakthrough data closely while Adams-Bohart model displayed great deviations. The regression coefficients of Yoon-Nelson model were higher (R^2>0.98) than those of Adams-Bohart model. These results confirmed that Yoon-Nelson model described the breakthrough data satisfactorily. Consequently, it was concluded that the rate of decrease in the probability of an adsorbate molecule is proportional to the probability of adsorbate adsorption and the probability of adsorbent breakthrough on adsorbent. These results are consistent with others reported in literature [13].

3.3. Scale-up study

Scale-up test were conducted to determine if the bench-scale data obtained could accurately predict the performance of a scaled-up fixed-bed unit at different operational parameters. To achieve this, the bed depth service time (BDST) model was applied for predictions because it is the most widely acceptable model for this purpose [14]. The linear equation of BDST model is given as:

$$t = \frac{N_o Z}{C_o U} - \frac{1}{k_B C_o}\ln\left(\frac{C_o}{C_t} - 1\right) \quad (3)$$

where N_o (mg/mL) is the capacity, k_B (mL/mg.min) is the rate constant, U is the linear velocity (cm/min), and Z (cm) is the bed depth. A plot of t versus Z should yield a straight line, from which values of N_o and k_B can be extracted from the slope and intercept.

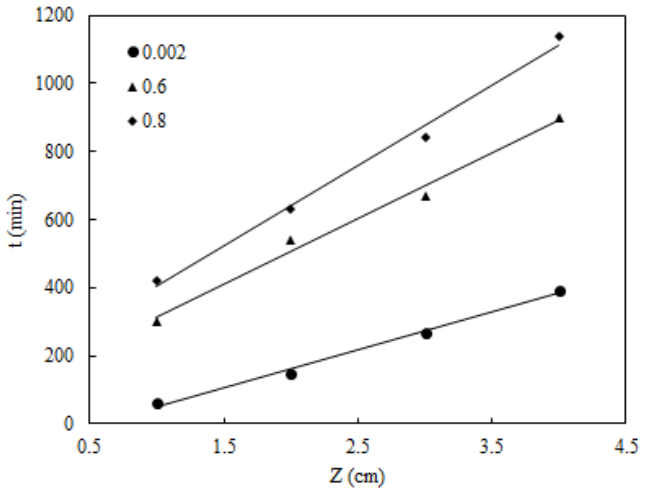

Fig. 5. The iso-removal lines at different C_t/C_o ratios

Figure 5 shows the iso-removal lines for different C_t/C_o ratios (0.002, 0.6, and 0.8), obtained after plotting Eq. (3) while Table 1 gives the summary of parameters calculated from the BDST plots. All iso-removal lines were linear with high regression coefficient values (R^2>0.98) which suggested better fitting of the experimental data with the BDST model. The k_B values decreased with increased effluent concentration while N_o values increased with effluent Mn (II) concentration. Moreover, the slope and intercept were significantly affected by change in effluent concentration. Thereafter, BDST parameters were used to predict saturation time at breakthrough for 75 mg/L influent concentration at constant flowrate (3.33 mL/min) and bed depth (20 mm). The predicted saturation time was 108 min, which was very close to the experimentally obtained saturation time (95 min). The results confirm the suitability of the BDST model in predicting the performance of a fixed-bed column packed with B/MeOx/H adsorbent material for Mn (II) clean-up.

Table 1. A summary of calculated parameters from the BDST model (C_o= 50 mg/L, Q= 3.33 mL/min)

C_t/Co	a (min/cm)	b (min)	k_B x10^{-3} (L/mg.min)	N_o x10^3 (mg/L)	R^2
0.002	111	60	2.07	2.941	0.9956
0.6	193	-120	0.07	5.114	0.9882
0.8	237	-165	0.17	6.281	0.9914

4. Conclusions

The present study investigated the ability of B/MeO$_x$/H hydrogel beads to continuously decontaminate Mn (II)-polluted water in a fixed-bed column. SEM and EDX characterization confirmed rough morphologies and the presence of all individual components. Increasing bed depth increased the breakthrough time and bed saturation time while it was the opposite with the flow rate. Linear regressions indicated that the Mn (II) breakthrough data can sufficiently be described by the Yoon-Nelson model. Furthermore, the predicted performance according to bed depth service time (BDST) model were in agreement with experimental values. This confirmed that BDST model can be used for scale-up studies under different operational conditions. The results provides important insights into the remediation of Mn (II)-contaminated water using B/MeO$_x$/H hydrogel adsorbent.

Acknowledgement

Authors acknowledge Rand Water South Africa through the Rand Water Chair in Water Utilization for financial support towards this project.

References

[1] A. Omri, M. Benzina, "Removal of manganese(II) ions from aqueous solutions by adsorption on activated carbon derived a new precursor: Ziziphus spina-christi seeds," *Alexandria Eng. J.*, vol. 51, pp. 343-350, 2012.

[2] A.M. Silva, E.C. Cunha, F.D. Silva, V.A. Leao, "Treatment of high-manganese mine water with limestone and sodium carbonate," *J Cleaner Prod.*, vol. 29-30, pp. 11-19, 2012.

[3] N. Li, J. Zhao, Z. Jiang, B. Cao, Y. Lu, D. Shan, Y. Zhang, "Continuous manganese(II) ions removal from aqueous solutions using rice husk ash-packed column reactor," *Desalination Water Treat.*, vol. 21, pp. 916-924, 2016.

[4] F. Ji, C. Li, J. Xu, P. Liu, "Dynamic adsorption of Cu(II) from aqueous solution by zeolite/cellulose acetate blend fiber in fixed-bed," *Colloids Surf. A: Physicochem. Eng. Aspects*, vol. 434 (2013), pp. 88-94, 2013.

[5] A. Tripathi, M.R. Ranjan, "Heavy Metal Removal from Wastewater Using Low Cost Adsorbents," *Bioremed. Biodegrad.*, vol. 6 (2015). DOI: 10.4172/2155-6199.1000315

[6] S.A. Al-Jlil, "Removal of heavy metals from industrial wastewater by adsorption using local bentonite clay and roasted date pits in Saudi Arabia," *Trends Appl. Sci. Res.*, vol. 5, pp.138-145, 2010.

[7] K.G. Akpomie, F.A. Dawodua, "Potential of a low-cost bentonite for heavy metal abstraction from binary component system," *Beni-Suef Univ. J. Basic Appl. Scie.*, vol.4, pp. 1-13, 2015.

[8] A.M. Mahmoud, F.A. Ibrahim, S.A. Shaban, N.A. Youssef, "Adsorption of heavy metal ion from aqueous solution by nickel oxide nano catalyst prepared by different methods," *Egypt. J. Petrol.*, vol. 24, pp. 27-35, 2015.

[9] D. Zhou, D.G. Kim, S.O. Ko, "Heavy metal adsorption with biogenic manganese oxides generated by Pseudomonas putida strain MnB1," *J. Ind. Eng. Chem.*, vol. 24, pp. 132-139, 2015.

[10] J.A. Alexander, A. Surajudeen, E.N.U. Aliyu, A.U. Omeiza, M.A.A. Zaini, "Multi metals column adsorption of lead(II), cadmium(II) and manganese(II) onto natural bentonite clay," *Water Sci. Technol.*, vol. 76, pp. 7-8, 2017.

[11] F.W. Sousa, A.G. Oliveira, J.P. Ribeiro, M.F. Rosa, D. Keukeleire, R.F. Nascimento,"Green coconut shells applied as adsorbent for removal of toxic metal ions using fixed-bed column technology," *J. Environ. Manage.*, vol. 91, pp. 1634-1640, 2010.

[12] S. Vilvanathan, S. Shanthakumar, "Continuous biosorption of nickel from aqueous solution using Chrysanthemum indicum derived biochar in a fixed-bed column," *Water Sci. Technol.*, vol 76, pp. 1895-1906, 2017.

[13] M. Bhaumik, K. Setshedi, A. Maity, M.S. Onyango, "Chromium(VI) removal from water using fixedbed column of polypyrrole/Fe_3O_4 nanocomposite," *Sep. Purif. Technol.*, vol. 110, pp. 11–19, 2013.

[14] A. Saravanan, P.S. Kumar, M. Yaswanthraj, "Modeling and analysis of a packed-bed column for the effective removal of zinc from aqueous solution using dual surface-modified biomass," *Part. Sci. Technol.*, 2017. https://doi.org/10.1080/02726351.2017.1329243.